Asymmetrical Planetary Nebulae II: From Origins to Microstructures
ASP Conference Series, Vol. XXX, 2000
J.H. Kastner, N. Soker, & S. Rappaport, eds.

MHD Models for PNe

G. García-Segura, J. Franco, J. A. López

Instituto de Astronomía-UNAM, Mexico

N. Langer

Institut für Physik, Universität Potsdam, Germany

M. Różyczka

N. Copernicus Astronomical Center and Interdisciplinary Center for Mathematical and Computational Modeling, Poland

Abstract. In this work, we address several controversial features that appear in Planetary Nebulae which are easily solved by the inclusion of MHD effects. These features include the presence of axisymmetric flows, confinement of flows, linearly encreasing kinematics of collimated outflows and asymmetrical morphologies such as point-symmetric nebulae.

1. Introduction

Planetary nebulae (PNe) display a rich variety of shapes, and have been cataloged in a series of morphological classes: bipolar, elliptical, point-symmetric, irregular, spherical and quadrupolar (Chu, Jacoby & Arendt 1987; Schwarz, Corradi & Melnick 1992; Stanghellini, Corradi & Schwarz 1993; Manchado et al. 1996ab). In contrast, except for a few cases, dust shells around AGB stars do not show signs of asphericity (Bujarrabal & Alcolea 1991; Kahane & Jura 1994). Thus, during the transition from the AGB to the post-AGB phase, one or more physical processes responsible for the shape of these objects must be initiated. The origin of aspherical nebulae still remains as one of the fundamental problems of PNe formation and evolution (see reviews by Pottasch 1984 and by Iben 1993).

Numerical simulations that reproduce the shapes of planetary nebulae (PNs) have helped to understand or give insights into the basic physics acting behind the formation of the different morphologies that are commonly observed in PNs. The two-wind model proposed by Kwok, Purton & Fitzgerlad (1978) has been applied and refined in a number of numerical simulations based on hydrodynamic models (e.g. Khan & West 1985; Mellema, Eulderink & Icke 1991; Frank & Mellema 1994; Dwarkadas, Chevalier & Blondin 1996).

The main nebular morphologies are usually well reproduced in the hydrodynamic models, however, the production of jets and ansae have met with certain difficulties; in particular, fast winds do not tend to converge into stable structures to form ansae and jets (e.g. Dwarkadas & Balick 1997).

On a somewhat different approach, Chevalier & Luo (1994) have explored the effects of a rotating star with a magnetized wind on the formation of aspherical bubbles. Following this scheme, Różyczka & Franco (1996) and García-Segura et al. (1997, 1999), performed 2-D MHD simulations of this magnetized wind in cylindrical and spherical calculations, respectively, showing that magnetic tension may indeed be responsible for the generation of jets in PNs. Recently, García-Segura (1997) presented full 3-D MHD models of PNs where jets and ansae are convincingly reproduced as the result of magnetic collimation of the post-AGB wind.

A particularly intriguing case in PNs morphologies are those that display point-symmetric structures. Point-symmetry has been now recognized in a wide variety of PNs (Manchado et al 1996; Guerrero, Vázquez & López 1999). In some instances, where reliable kinematical information is available, the presence of bipolar, rotating, episodic jets or BRETS have been inferred to explain similar structures (c.f. López 1997).

Why do we care about Point-Symmetry? At first view, the point-symmetric morphological class does not look very important. But, a careful inspection to the statistically, complete sample of the IAC morphological catalog (Manchado et al.1996) reveals 40 objects with some degree of point-symmetric features, which represent the 19% of the total list (215) with a well defined morphology, i.e., we have not taken into account those objects classified as S for stellar or G for gaussian profiles. Note that many of these nebulae are not classified as point-symmetric. In fact, they have been well classified inside the categories of bipolars and ellipticals, such as the case of the Dumbel nebula. This fact points in the direction that the point-symmetry is a common feature related to any morphological class, instead of a separate group (the authors of the IAC catalog also agree in this point; Manchado 1998, private communication). Bipolar nebulae which present clear point-symmetric structures in this sample include M 1-59, PC 20, K 3-4, K 3-34, He 2-437, K 3-58, K 4-55, We 1-11, K 3-83, M 2-52, K 3-91, NGC 650-51, K 3-72, M 1-8; while ellipticals include M 2-40, IC 1295, M 3-34, He 2-429, NGC 6853, K 4-37, Hu 1-2, M 1-79, A 80, M 2-53, M 2-55, Hu 1-1, K 3-90, K 3-92, M 3-3. Five nebulae classified as point-symmetric as well as six quadrupolar nebulae are not listed for obvious reasons. Such a large fraction of the sample (19%) suggest that the reason which produces point-symmetry should be very common.

In this paper, we focus on individual features that are easily solved by MHD effects. In § 2 we discuss the production of axisymmetric flows. § 3 describes the confinement of flows and the production of jets and ansae. § 4 address the linearly encreasing kinematics of the collimated outflows and § 5 give solutions for the special case of point-symmetric nebulae.

2. Axisymmetric flows

Axisymmetric flows can be produced by a magnetized wind with or without the existence of an equatorial density enhacement (EDE) (see García-Segura et al. 1999 for examples). The magnetic field at the surface of a post-AGB star can be transported out by its wind, like in the solar case. Because of stellar rotation, the magnetic field in the wind is dominated by a toroidal component. The resulting toroidal field has a magnetic tension associated with it (Chevalier & Luo 1994; Contopoulos 1995). Thus, the general effect of the magnetic tension is the elongation of the nebula in the polar direction. The mechanism responsible for the elongation was described by Różyczka & Franco (1996), and only the basic points are listed here. First, the outer part of the magnetized shocked wind region becomes magnetically rather than thermally supported, i.e. the magnetic energy density becomes larger than the thermal energy density. The latter decreases due to the expansion of the nebula and due to the fact that work must be done against the tension of the toroidal field. Second, the tension of the toroidal field slows down the expansion in the direction perpendicular to the symmetry axis, while the expansion in the direction parallel to the axis proceeds almost unimpeded. Third, a flow in the shocked wind region toward the symmetry axis is initiated, leading to the formation of stagnation regions at the rotational axis. Note that at the reverse shock, there is a large gradient in the magnetic pressure because the toroidal field at the rotation axis is nule in the free expanding wind.

Unfortunately, there is no information about stellar magnetic fields at the surfaces of post-AGB stars in one of the most interesting regions of the HR diagram, between the AGB phase and the white dwarf phase. Reid et al.(1979) found strong circular polarization in the OH masers from U Ori and IRC +10420. The OH masers indicate fields of about 10 milligauss emanating from regions of about 10^{15} cm from the star. They suggest that the field strenghts at the stellar surfaces are on the order of 10 and 100 Gauss respectively. White dwarfs are known to have fields of up to $10^7 - 10^8$ Gauss (Schmidt 1989). So, stellar field intensities between the solar value ($B_{\rm s}$ = 2 Gauss, in average) and 10^8 Gauss are acceptable for modeling. Note that observations for the detection of magnetic fields in the swept-up shells of PNe (eg Terzian 1989) have been tried, but however, they give us very little information about the field intensity of the nucleus, since that diluted field will correspond to the already expanded and compressed AGB gas.

3. Confinement of flows: jets and ansae

Although the hoop stress is always present in this type of flows, not always the conditions are in favor to form observable jets. Such a case is computed in model E2 (Fig. 1), in which the mass-loss rate of the fast wind has been decreased by an order of magnitude respect to model E1. In such conditions, the fast wind piles up at the poles, but the radiative cooling, proportional to n^2, is not sufficiently strong to allow the formation of visible jets, and ansae-like structures are formed instead.

The result of varying the mass loss rate of the fast wind from large values to lower values is quite important for jet formation/detection. Note that, since we are very limited by numerical resolution, these numbers should be taken as estimative values for the mass loss rates, because cooling regions are not really resolved.

Figure 1 shows the appreciable difference between models E1, E2, and E3. The polar, piled-up gas in model E1 (higher value of $\dot{M}$) is able to cool down efficiently in a dynamical time scale comparable to the computed time. This

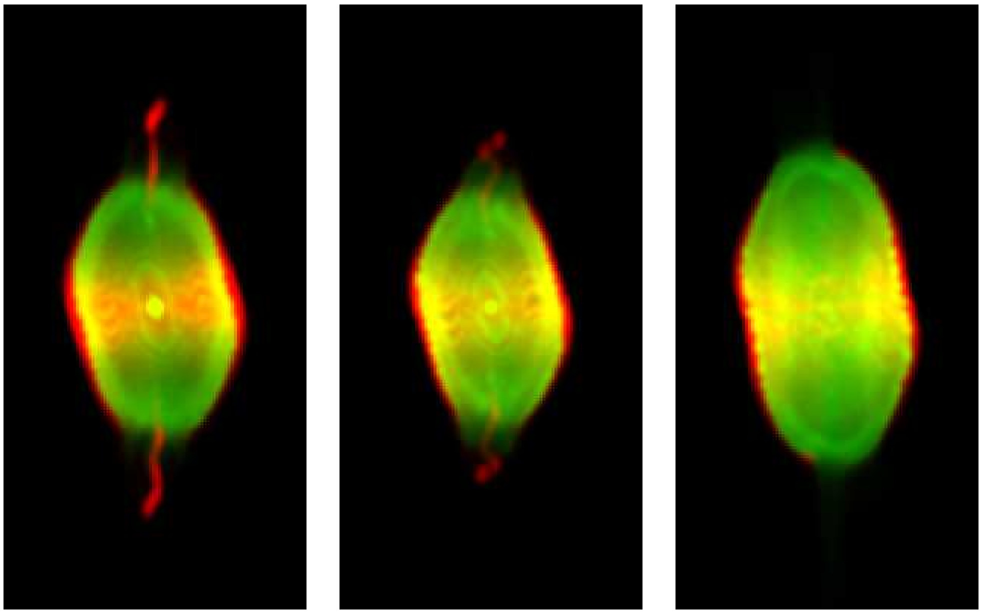

Figure 1. Two-color, composite, synthetic images of the models E1 (1600 yr; $\dot{M} = 10^{-7}$ $M_\odot$)(left), E2 (1550 yr; $\dot{M} = 10^{-8}$ $M_\odot$)(middle) and E3 (2000 yr; $\dot{M} = 10^{-9}$ $M_\odot$)(right)

feature results in "easily" detectable jets. In model E2 (moderate $\dot{M}$) the cooling is less efficient but still present, giving rise to the formation of ansae. Model E3 does not show any apparent signs of piled-up gas. Since these models have energy conserving dynamics (as imposed by the magnetic pressure) rather than momentum conserving, these estimations for the mass loss rates are quite independent of the terminal wind velocities. Note that, in the absence of magnetic field, winds of the order of 100 km s^{-1} have strongly radiative terminal or reverse shocks (see for example Frank et al. 1996), and the radiative conditions are strongly dependent of the wind velocity and not only of the mass loss rate.

4. Linearly encreasing kinematics of the collimated outflows

A comparison of the morphologies in observed nebulae with those resulting from the computed models provides a first test of the model goodness. A second verification can be performed with the kinematics of nebulae and, specially, with the fast outflows/jets that have been reported for several PNe during this last decade. Examples with fast outflows ($\sim$ 500 km s^{-1} or higher) are He 3-1475 (Riera et al.1995) and MyCn 18 (Bryce et al.1997). The observed large velocity values are hardly explained by invoking only hydrodynamical effects (Frank et al. 1996), since they are above the critical velocity of $\sim$ 150 km s^{-1} for which interstellar shocks become adiabatic. Magnetohydrodynamical effects, on the other hand, are very efficient in forming these fast collimated outflows, as discussed in Section 3.

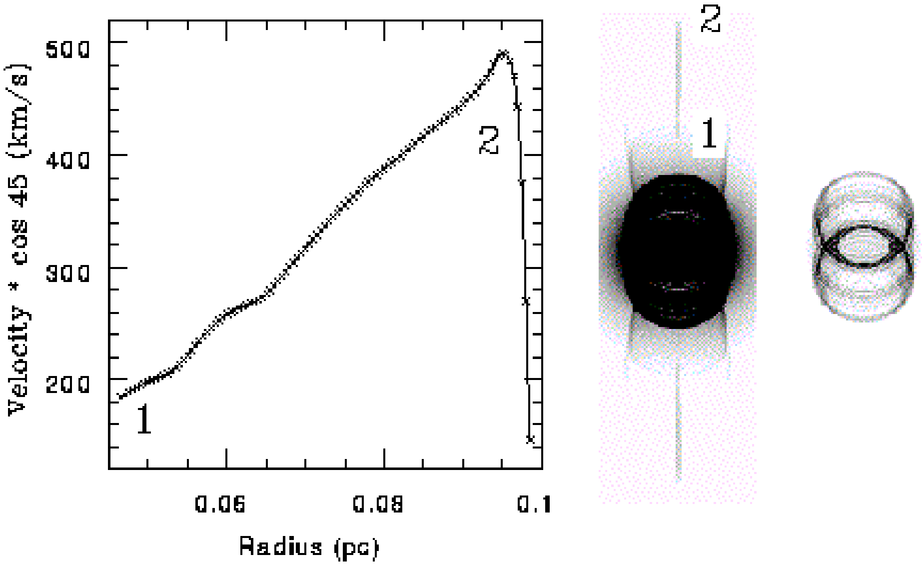

Figure 2. The projected expansion velocity of the model U jet tilted 45° from the plane of the sky is shown on the left. Crosses represent grid point values, and the solid line the interpolation. The labels 1 and 2 delimit an artificial slit along the jet shown in the middle panel. The middle and right panels are linear grey scale representations of the emission measure of model U.

In order to verify if the MHD models can reproduce the range of observed velocities, Figure 2 shows the expansion velocity of the jet that appears in model U (GGS et al 1999) as it should be observed with a synthetic slit covering only the jet positions (1–2 on the figure). The model has been tilted 45° for a qualitative comparison with MyCn 18. The left panel of Figure 2 agrees quite well with figure 3a in Bryce et al. (1997), although the model was not specifically intended to reproduce this nebula. The most remarkable feature is the approximately linear increase of the expansion velocity along the jet, that matches the actual echelle observations. This accelerative behavior is produced by the relaxation of the magnetic pressure in the shocked region. For completness, the middle and right panels in Figure 2 display two synthetic images of the emission measure of the gas, which can be also compared with figure 1 in Bryce et al. (1997). The qualitative agreement is notorious.

5. Solutions for point-symmetry

Since the toroidal magnetic field carried out by the wind is always perpendicular to the rotation axis of the central star, it is now tempting to include a precession (scenario I) or a steady tilt (scenario II) in the rotational axis. In both cases, it is easy to imagine the topology of the magnetic field lines in such scenarios, i.e., multiple magnetic rings centered along the spin axis of the star.

In scenario I, in order to reproduce point-symmetric structures, a wide binary nucleus was considered and the magnetic collimation axis (i.e. the rotation

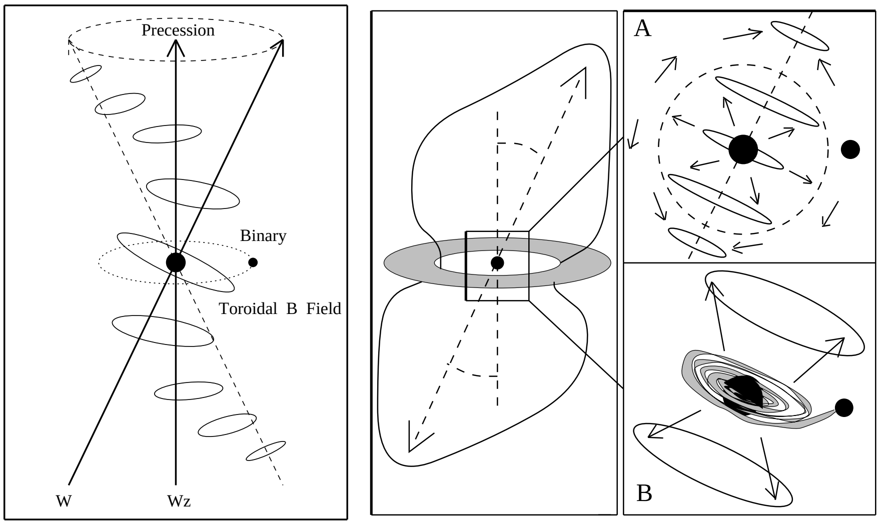

Figure 3. (Left: scenario I) Magnetic field configuration of the wind emerging from a precessing star. The field is always perpendicular to the rotation axis. The rotation axis of the star is labeled with W, while the axis of precession is W_z. (Right: scenario II) The magnetic collimation axis (dashed line) is tilted with respect to the symmetry axis of the bipolar wind outflow, which is perpendicular to the equatorial density enhancement

axis of the primary star) was assumed to precess, with a period of the same order of the kinematic age of the nebulae ($\sim 10^3$ yr).

In scenario II, instead of invoking an active rotation of the magnetically collimated outflow, a misaligned configuration is produced by introducing a steady tilt of the magnetic collimation axis with respect to the bipolar/elliptical wind outflow. Hence, this is a particular case of scenario I, in which the precession period is nule or much larger than the kinematic age of the nebula.

The MHD models are sketched in Figure 3. Here, either a rotating star with a magnetized wind member of a wide binary system (A) or the X-wind from an accretion disk (B) produces the outflowing magnetized wind, in which the toroidal component of the magnetic field is dominant respect to the poloidal contribution at large distances. Thus, the same physics can be applied in both cases.

In order to illustrate how the precession (scenario I) can produce interesting effects, we have computed a model (Figure 4, left) with a period of precession of 1300 yr, and with a precession angle of 10°.

In order to have a general picture of the effect caused by the tilt (scenario II), we have computed several models in which the tilt angle varies from low values, 5°, middle values, 15° and large values, 45° (Figure 4, middle and right).

The dynamics of the bubbles in such conditions are quite complex and the limited resolution of the models hinder a full, quantitative description. Nevertheless, the effect of the tilt can be summarize qualitatively as follows.

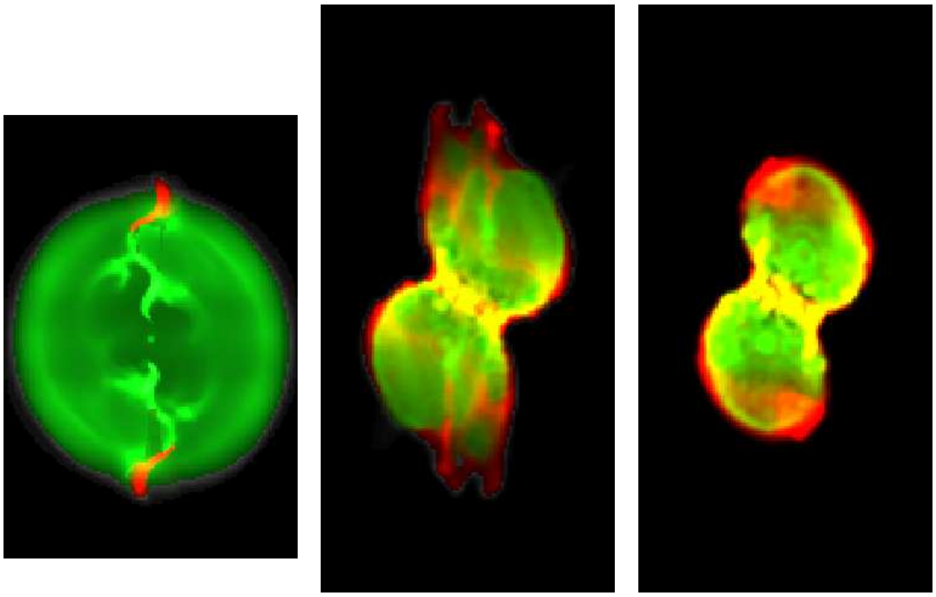

Figure 4. (Left: scenario I) An example of a calculation which includes stellar precession ($t = 1300$ yr). (Middle and right: scenario II) Examples of two calculations which include and steady tilt of 45°

At the beginning of every simulation, the spherically symmetric shocked flow is driven by the magnetic pressure gradient after crossing the reverse or terminal shock and is launched in the z direction on both sides of the wind source region. Since the magnetic field is toroidal, the magnetic pressure is nule towards the z axis in the free expanding wind (but not in the shocked region), while it is maximum in the equatorial plane, consequently building a large pressure gradient. Gradually, the flow notices the effect of the EDE and is deflected perpendicular to it. The magnetically pressurized bubble is distorted, and the flow, which now follows the tendency of the bipolar cavity, pushes and deflects the column of gas in which the hoop stress is larger. When this column is dense enough, the formed jets are deflected an acquire the appearance of precessing jets, which eventually will collide with the bipolar cavity. Thus, there are two competing effects, one is the tendency of the gas to flow perpendicular to the EDE, and the other is the tendency of the gas to flow parallel to the z axis as imposed by the magnetic pressure and the hoop stress. When the tilt is nule, i.e., when both effects do not compete with each other, the bubble acquires the largest expansion velocity at the polar regions.

Acknowledgments. G.G.S. is grateful to A. Manchado and M. Peimbert for useful discussions. All the computations were done with ZEUS-3D and performed at Instituto de Astronomía-UNAM. We thank Michael L. Norman and the Laboratory for Computational Astrophysics for the use of ZEUS-3D.

References

Bryce, M., López, J. A., Holloway, A. J., & Meaburn, J. 1997, ApJ, 487, L161

Bujarrabal, V. & Alcolea J., 1991, A&A, 251, 536

Chevalier, R. A., & Luo, D. 1994, ApJ, 421, 225

Chu, Y.-H., Jacoby, G. H. & Arendt, R. 1987, ApJS, 64, 529

Contopoulos, J. 1995, ApJ, 450, 616

Dwarkadas, V. V., Chevalier, R. A. & Blondin, J.M. 1996, ApJ, 457, 773

Dwarkadas, V. V. & Balick, B. 1997, BAAS, 191, #15.05

Frank, A. & Mellema, G. 1994, A&A, 289, 937

Frank, A., Balick, B., & Livio, M. 1996, ApJ, 471, L53

García-Segura, G. 1997, ApJL, 489, L189

García-Segura, G., Langer, N., Różyczka, M., & Franco, J. 1999, ApJ, 517

García-Segura, G., Langer, N., Różyczka, M., Mac Low, M.-M., & Franco, J. 1997, in IAU Symp. No 180 "Planetary Nebulae", eds. Habing & Lamers, (Kluwer Academic Publishers, Dordrecht), in press

Guerrero, M.A., Vázquez, R., & López, J.A. 1998, ApJ, 117, 967

Iben, I. Jr. 1993, in IAU Symp. No 155 "Planetary Nebulae", ed. R. Weinberger and A. Acker, (Kluwer Academic Publishers, Dordrecht), 587

Kahane, C. & Jura M., 1994, A&A, 290, 183

Khan, F.D. & West, K. 1985, MNRAS, 212, 837

Kwok, S., Purton, C. R. & Fitzgerald, P. M. 1978, ApJ 219, L125

López, J. A. 1998, in IAU Symp. No 180 "Planetary Nebulae", eds. Habing & Lamers, (Kluwer Academic Publishers, Dordrecht), in press

Manchado, A., Guerrero, M., Stanghellini, L., & Serra-Ricart, M. 1996, "The IAC Morphological Catalog of Northern Galactic Planetary Nebulae", ed. Instituto de Astrofísica de Canarias

Manchado, A., Stanghellini, L., & Guerrero, M. 1996b, ApJL, 466, L95

Mellema, G., Eulderink, F. & Icke, V. 1991, A&A, 252, 718

Mellema, G., & Frank, A. 1997, MNRAS, in press

Pottasch, S. R. 1984, "Planetary Nebulae. A Study of Late Stages of Stellar Evolution", (D. Reidel Publishing Company, Dordrecht)

Reid, M. J., Moran, J. M., Leach, R. W., Ball, J. A., Johnston, K. J., Spencer, J. H., & Swenson, G. W. 1979, ApJL, 227, L89

Riera, A., García-Lario, P., Manchado, A., Pottasch, S. R., & Raga, A. C. 1995, A&A, 302, 137

Różyczka, M. & Franco, J. 1996, ApJL, 469, L127

Schmidt, G. 1989, in IAU Coll. 114, "White Dwarfs", ed. G. Wegner (Dordrecht, Kluwer), 305

Schwarz, H. E., Corradi, R. L. M., & Melnick, J. 1992, A&A Suppl, 96, 23

Stanghellini, L., Corradi, R. L. M. & Schwarz, H. E. 1993, A&A, 276, 463

Terzian, Y. 1989, in IAU Symp No 131, Planetary Nebulae, 17